

Stepwise Spectral Swapping with Three Neutrino Flavors

Huaiyu Duan,^{1,*} George M. Fuller,^{2,†} and Yong-Zhong Qian^{3,‡}

¹*Institute for Nuclear Theory, University of Washington, Seattle, WA 98195*

²*Department of Physics, University of California, San Diego, La Jolla, CA 92093-0319*

³*School of Physics and Astronomy, University of Minnesota, Minneapolis, MN 55455*

(Dated: November 4, 2018)

We develop a framework for studying collective three-flavor neutrino oscillations based on the density matrix formalism. We show how techniques proven useful for collective two-flavor neutrino oscillations such as corotating frames can be applied readily to three-flavor mixing. Applying two simple assumptions and the conservation of two “lepton numbers” we use this framework to demonstrate how the adiabatic/precession solution emerges. We illustrate with a numerical example how two stepwise spectral swaps appear naturally if the flavor evolution of the neutrino gas can be described by such a solution. For the special case where mu and tau flavor neutrinos are equally mixed and are produced with identical energy spectra and total numbers, we find that one of the spectral swaps in the three-flavor scenario agrees with that in the two-flavor scenario when appropriate mixing parameters are used. Using the corotating frame technique we show how the adiabatic/precession solution can obtain even in the presence of a dominant ordinary matter background. With this solution we can explain why neutrino spectral swapping can be sensitive to deviations from maximal 23-mixing when the “mu-tau” matter term is significant.

PACS numbers: 14.60.Pq, 97.60.Bw

I. INTRODUCTION

It has long been recognized that, in addition to the conventional Mikheyev-Smirnov-Wolfenstein (MSW) effect [1, 2, 3], neutrino self-coupling can be important for neutrino flavor evolution when neutrino number densities are large [4, 5, 6, 7, 8, 9, 10, 11, 12, 13, 14, 15]. Recently two-flavor neutrino oscillations in the core-collapse supernova environment have been intensively investigated [16, 17, 18, 19, 20, 21, 22, 23, 24]. These studies show that supernova neutrinos can indeed experience collective flavor evolution because of neutrino self-coupling, even when the neutrino self-coupling is subdominant compared to the MSW potential [16].

An important result is that collective two-flavor neutrino oscillations can exhibit “stepwise spectral swaps” or “spectral splits” in the final neutrino energy spectra when the neutrino number density slowly decreases from a high value, where neutrinos experience synchronized oscillations [12], towards zero (see, e.g., Ref. [18]). When this occurs, ν_e ’s appear to swap their energy spectra with ν_x ’s at energies below or above (depending on the neutrino mass hierarchy) a transition energy $E_{2\times 2}^s$ (where the superscript “s” can stand either for “swapping point” or “splitting point”). Here ν_x is some linear combination of ν_μ and ν_τ . The phenomenon of spectral swapping is present in both the “single-angle approximation”, where flavor evolution along various neutrino trajectories is assumed to be the same as that along a representative tra-

jectory (e.g., the radial trajectory), and the “multi-angle approximation”, where flavor evolution along different trajectories is independently followed [17]. For the inverted neutrino mass hierarchy, it also has been found that stepwise neutrino spectral swapping is essentially independent of the 2×2 effective vacuum mixing angle when this angle is small (see, e.g., Ref. [22]).

Collective two-flavor neutrino oscillations are best understood with the help of neutrino flavor polarization vectors [7] or neutrino flavor isospins [16]. Using the spin analogy, one can represent the flavor content of a neutrino mode by a spin vector in flavor isospace. In this analogy, the matter effect is described as a spin-field coupling, and the neutrino self-coupling is described as spin-spin coupling. The phenomenon of spectral swapping is a result of collective precession of all neutrino flavor isospins with a common angular velocity Ω_{pr} at any given neutrino number density [17, 21]. This collective precession of neutrino flavor isospins is described the two-flavor adiabatic/precession solution [25, 26]. In this solution, all neutrino flavor isospins stay aligned or antialigned with a total effective field in a reference frame that rotates with angular velocity Ω_{pr} . Numerical simulations have shown that, in the supernova environment, neutrinos can first experience collective MSW-like flavor transformation (in which the MSW effect is enhanced by neutrino self-coupling) and then subsequently the adiabatic/precession solution [27].

In the real world, however, there are three active neutrino flavors. Some limited progress has been made on understanding collective three-flavor neutrino oscillations. The first fully-coupled simulation of three-flavor neutrino oscillations in the supernova environment showed a spectral swapping phenomenon similar to the two-flavor scenario except possibly with two swaps [28].

*Electronic address: Huaiyu.Duan@mailaps.org

†Electronic address: gfuller@ucsd.edu

‡Electronic address: qian@physics.umn.edu

Another simplified numerical study with a single neutrino energy bin [29] reveals that collective neutrino oscillations can be sensitive to deviations from maximal 23-mixing when there is a dominant “mu-tau” term arising from a high order contribution from virtual μ ’s and τ ’s (e.g., Refs. [4, 30, 31]). Ref. [32] has extended the neutrino flavor polarization vector notation to the three-flavor scenario and discussed the collective three-flavor oscillations as “factorization” of two two-flavor oscillations.

In this paper we develop a framework for studying collective three-flavor neutrino oscillations based on the density matrix formalism. Using this framework we find a generalized three-flavor adiabatic/precession solution and show how stepwise spectral swapping can appear as a natural result of such a solution.

The rest of this paper is organized as follows. In Sec. II we develop a framework centered around a 3×3 reduced neutrino flavor density matrix. This density matrix is equivalent to an 8-component neutrino flavor vector, a generalization of neutrino flavor isospin and similar to the Bloch vector used in Ref. [32]. We show how techniques important in studying collective two-flavor oscillations such as corotating frames can be applied in the framework. In Sec. III we demonstrate how the three-flavor adiabatic/precession solution can be found using two simple assumptions and the conservation of two “lepton numbers”. We also illustrate with a numerical example how two spectral swaps can form from the adiabatic/precession solution when the total neutrino number density vanishes. In Sec. IV we employ the corotating frame technique and show that the adiabatic/precession solution obtains even in the presence of a dominant matter background. In particular, we show that, in the presence of a large mu-tau term, neutrino spectral swapping becomes sensitive to deviations from maximal 23-mixing. In Sec. V we give our conclusions.

II. EQUATIONS OF MOTION

A. Density Matrix Description

The flavor content of a neutrino (antineutrino) mode with momentum \mathbf{p} is generally described by density matrix $\rho_{\mathbf{p}}$ ($\bar{\rho}_{\mathbf{p}}$) [7]. The diagonal elements of a density matrix are the occupation numbers of the neutrino eigenstates in a particular basis, and the off-diagonal elements contain the phase information relating to neutrino mixing. For a neutrino pure state described by flavor wavefunction

$$\psi_{\nu_{\mathbf{p}}} = \begin{pmatrix} a_{\nu_1} \\ a_{\nu_2} \\ a_{\nu_3} \end{pmatrix}, \quad (1)$$

the density matrix is

$$\rho_{\mathbf{p}} = n_{\nu_{\mathbf{p}}} \begin{pmatrix} |a_{\nu_1}|^2 & a_{\nu_1} a_{\nu_2}^* & a_{\nu_1} a_{\nu_3}^* \\ a_{\nu_2} a_{\nu_1}^* & |a_{\nu_2}|^2 & a_{\nu_2} a_{\nu_3}^* \\ a_{\nu_3} a_{\nu_1}^* & a_{\nu_3} a_{\nu_2}^* & |a_{\nu_3}|^2 \end{pmatrix}, \quad (2)$$

where $n_{\nu_{\mathbf{p}}}$ is the neutrino number density in momentum mode \mathbf{p} , and $a_{\nu_i(\nu_2, \nu_3)}$ are the amplitudes for the neutrino to be in the corresponding vacuum mass eigenstates. With this notation we have normalization

$$\sum_{i=1,2,3} |a_{\nu_i}|^2 = 1. \quad (3)$$

The density matrix $\bar{\rho}$ for an antineutrino pure state is defined similarly.

In this paper we will assume that the CP -violating phase is $\delta = 0$. A brief discussion of the effect of a non-vanishing CP phase is given in Sec. V. Because we are only interested in neutrino flavor transformation, we will assume that neutrinos are free streaming except for forward scattering on the background medium. For now we also will assume that there is no ordinary matter background. For this case it is most convenient to work in the vacuum mass basis. This basis is implicitly adopted in all the following discussions except for Sec. IV, where we will discuss the effects of the ordinary matter potential. To simplify the problem even further, we will assume that the neutrino gas is isotropic and uniform. This corresponds to the “single-angle approximation” in numerical simulations of flavor oscillations of supernova neutrinos. It has been shown numerically [17, 18, 23, 24] that both single-angle and multi-angle calculations produce similar neutrino spectral swaps.

For an isotropic and uniform neutrino gas confined in a fixed volume, the equations of motion (e.o.m.) for neutrino density matrix $\rho_{\mathbf{p}}$ are

$$i\dot{\rho}_{\mathbf{p}} = [\mathbf{H}_{\mathbf{p}}, \rho_{\mathbf{p}}]. \quad (4)$$

Here the Hamiltonian for neutrino mode \mathbf{p} is

$$\mathbf{H}_{\mathbf{p}} = \mathbf{H}_{\mathbf{p}}^{\text{vac}} + \sqrt{2}G_F \int \frac{d^3\mathbf{q}}{(2\pi)^3} (\rho_{\mathbf{q}} - \bar{\rho}_{\mathbf{q}}^*), \quad (5)$$

where G_F is the Fermi constant, and the vacuum term in the Hamiltonian is

$$\mathbf{H}_{\mathbf{p}}^{\text{vac}} = \frac{1}{2|\mathbf{p}|} \text{diag}(m_1^2, m_2^2, m_3^2) \quad (6)$$

with m_i^2 being the mass-squared eigenvalues corresponding to neutrino vacuum mass eigenstates $|\nu_i\rangle$. For antineutrino density matrix $\bar{\rho}_{\mathbf{p}}$ one has

$$i\dot{\bar{\rho}}_{\mathbf{p}} = [\bar{\mathbf{H}}_{\mathbf{p}}, \bar{\rho}_{\mathbf{p}}], \quad (7)$$

with the Hamiltonian defined as

$$\bar{\mathbf{H}}_{\mathbf{p}} = \mathbf{H}_{\mathbf{p}}^{\text{vac}} + \sqrt{2}G_F \int \frac{d^3\mathbf{q}}{(2\pi)^3} (\bar{\rho}_{\mathbf{q}} - \rho_{\mathbf{q}}^*). \quad (8)$$

We note that Ref. [7] has defined the antineutrino density matrix as the complex conjugate of what one usually writes as a density matrix (i.e., $\bar{\rho}_{\mathbf{p}}^* \rightarrow \bar{\rho}_{\mathbf{p}}$). This notation leads to a slightly simpler version of the e.o.m. for both neutrinos and antineutrinos. However, for a vanishing CP phase, it is possible to treat neutrinos and antineutrinos on an equal footing and combine Eqs. (4) and (7) into a single expression, as has been done in Ref. [16] for the two-flavor mixing scenario. To see this, we note that a neutrino or antineutrino mode in an isotropic and uniform gas is completely characterized by

$$\omega(E) \equiv \mp \text{Tr}(\mathbf{H}_{\mathbf{p}}^{\text{vac}} \lambda_3) = \pm \frac{\Delta m_{21}^2}{2E}, \quad (9)$$

where $E = |\mathbf{p}|$ is the energy of the neutrino or antineutrino, upper (lower) signs are for neutrinos (antineutrinos), $\Delta m_{21}^2 = m_2^2 - m_1^2$ is approximately the solar mass-squared difference Δm_{\odot}^2 , and λ_3 is one of the Gell-Mann matrices λ_a ($a = 1, \dots, 8$). Because the number density for a neutrino (antineutrino) mode $\nu_{\mathbf{p}}$ ($\bar{\nu}_{\mathbf{p}}$) is conserved for a neutrino gas in a fixed volume, we can define the total neutrino number density

$$n_{\nu}^{\text{tot}} \equiv \int \frac{d^3\mathbf{q}}{(2\pi)^3} \text{Tr}(\rho_{\mathbf{q}} + \bar{\rho}_{\mathbf{q}}), \quad (10)$$

and the normalized distribution function is

$$f_{\omega} \equiv \frac{E^2}{2\pi^2 n_{\nu}^{\text{tot}}} \left| \frac{dE}{d\omega} \right| \times \begin{cases} \text{Tr}(\rho_{\mathbf{p}}) & \text{if } \omega > 0, \\ \text{Tr}(\bar{\rho}_{\mathbf{p}}) & \text{if } \omega < 0. \end{cases} \quad (11)$$

Using Eqs. (10) and (11) we can express the integral in Eq. (4) as

$$\int \frac{d^3\mathbf{q}}{(2\pi)^3} (\rho_{\mathbf{q}} - \bar{\rho}_{\mathbf{q}}^*) = n_{\nu}^{\text{tot}} \int_{-\infty}^{\infty} d\omega f_{\omega} \varrho_{\omega}. \quad (12)$$

In Eq. (12) we have defined the “reduced neutrino flavor density matrix” ϱ_{ω} for neutrino mode ω :

$$\varrho_{\omega} \sim \begin{cases} \rho_{\mathbf{q}} & \text{if } \omega > 0, \\ -\bar{\rho}_{\mathbf{q}}^* & \text{if } \omega < 0 \end{cases} \quad (13)$$

which has normalization

$$\text{Tr}(\varrho_{\omega}) = \begin{cases} +1 & \text{if } \omega > 0, \\ -1 & \text{if } \omega < 0. \end{cases} \quad (14)$$

Using Eqs. (4), (7) and (12) we find the e.o.m. for ϱ_{ω} :

$$i\dot{\varrho}_{\omega} = [\mathbf{H}_{\omega}, \varrho_{\omega}]. \quad (15)$$

The Hamiltonian for neutrino mode ω is

$$\mathbf{H}_{\omega} = \mathbf{H}_{\omega}^{\text{vac}} + \mu \varrho_{\text{tot}}, \quad (16)$$

where in the vacuum mass basis

$$\mathbf{H}_{\omega}^{\text{vac}} = -\omega \frac{\lambda_3}{2} - \kappa \frac{\lambda_8}{\sqrt{3}}. \quad (17)$$

Here we define

$$\mu \equiv \sqrt{2} G_{\text{F}} n_{\nu}^{\text{tot}}. \quad (18)$$

This parameter dictates the strength of neutrino self-coupling. The total neutrino flavor density matrix is defined to be

$$\varrho_{\text{tot}} \equiv \int_{-\infty}^{\infty} d\omega f_{\omega} \varrho_{\omega}. \quad (19)$$

In Eq. (16) we have left out the trace term for \mathbf{H}_{ω} (which is irrelevant for neutrino oscillations), and we have defined the oscillation parameter κ to be

$$\kappa(E) \equiv \mp \frac{\sqrt{3}}{2} \text{Tr}(\mathbf{H}_{\mathbf{p}}^{\text{vac}} \lambda_8), \quad (20a)$$

$$= \pm \frac{1}{2E} \left[m_3^2 - \frac{(m_1^2 + m_2^2)}{2} \right], \quad (20b)$$

where the upper (lower) signs are for neutrinos (antineutrinos). Because the atmospheric mass-squared difference Δm_{atm}^2 is much larger than Δm_{\odot}^2 , one has

$$m_3^2 - \frac{(m_1^2 + m_2^2)}{2} \simeq \pm \Delta m_{\text{atm}}^2, \quad (21)$$

where the plus (minus) sign is for the normal (inverted) neutrino mass hierarchy.

We note that f_{ω} does not change with time if there is no inelastic scattering of neutrinos. We also note that Eq. (15) is actually more generally valid than Eqs. (4) and (7) so long as the neutrino gas stays isotropic and uniform. For example, this would be true for an homogeneous and isotropic early universe, i.e., the Friedman solution. The “single-angle approximation” (see, e.g., Ref. [17]) for flavor evolution of supernova neutrinos is essentially equivalent to this scenario. For this case, the flavor content of a neutrino propagating along any trajectory at a given radius is assumed to be identical to that of a neutrino with the same energy propagating along a radial trajectory at the same radius. In this approximation the flavor evolution of neutrinos as a function of time t can be represented as the flavor evolution of neutrinos propagating along the radial trajectory as a function of radius r . In addition, one can define the effective total neutrino number density at each radius as

$$n_{\nu}^{\text{tot}} = \frac{D(r/R_{\nu})}{2\pi R_{\nu}^2} \sum_{\nu} \frac{L_{\nu}}{\langle E_{\nu} \rangle} \int_0^{\infty} dE f_{\nu}(E). \quad (22)$$

This takes account of both the geometric dilution and (partly) the anisotropy of supernova neutrinos. In Eq. (22) R_{ν} is the radius of the neutrino sphere, the geometric factor is

$$D(\xi) = \frac{1}{2} (1 - \sqrt{1 - \xi^{-2}})^2, \quad (23)$$

L_{ν} , $\langle E_{\nu} \rangle$ and $f_{\nu}(E)$ are the neutrino luminosity, average energy and normalized energy distribution function for species ν at the neutrino sphere, respectively, and the summation is over all neutrino species (including both neutrinos and antineutrinos).

B. Flavor Vector Description

The flavor polarization vector \mathbf{P} [7] and neutrino flavor isospin \mathbf{s}_ω [16] are important techniques that have been used extensively to describe the flavor mixing of neutrinos in two-flavor mixing scenarios. These notations have helped in visualizing and giving insights into the problem of collective neutrino oscillations.

To generalize these notations to the 3×3 case, we note that a 3×3 Hermitian matrix \mathbf{A} can be expressed as the linear combination of the identity matrix \mathbf{I} and Gell-Mann matrices λ_a :

$$\mathbf{A} = \frac{1}{3}\text{Tr}(\mathbf{A})\mathbf{I} + \sum_a A^{(a)} \frac{\lambda_a}{2}, \quad (24)$$

where

$$A^{(a)} \equiv \text{Tr}(\mathbf{A}\lambda_a) \quad (25)$$

can be viewed as the a 'th component of an 8-dimensional vector \mathbf{A} . In particular, “flavor vector”

$$\boldsymbol{\varrho}_\omega = (\varrho_\omega^{(1)}, \dots, \varrho_\omega^{(8)})^T \quad (26)$$

is the generalized version of neutrino flavor isospin \mathbf{s}_ω .¹

Because $\text{Tr}(\varrho_\omega)$ is fixed by the normalization condition in Eq. (14), flavor vector $\boldsymbol{\varrho}_\omega$ is fully equivalent to the density matrix ϱ_ω . In particular, the number densities of ν_1 , ν_2 and ν_3 in mode ω can be expressed in terms of $\varrho_\omega^{(3)}$ and $\varrho_\omega^{(8)}$:

$$n_{\nu_1}(\omega) = n_\nu^{\text{tot}} f_\omega \left(\frac{1}{3} + \frac{1}{2}\varrho_\omega^{(3)} + \frac{1}{2\sqrt{3}}\varrho_\omega^{(8)} \right), \quad (27a)$$

$$n_{\nu_2}(\omega) = n_\nu^{\text{tot}} f_\omega \left(\frac{1}{3} - \frac{1}{2}\varrho_\omega^{(3)} + \frac{1}{2\sqrt{3}}\varrho_\omega^{(8)} \right), \quad (27b)$$

$$n_{\nu_3}(\omega) = n_\nu^{\text{tot}} f_\omega \left(\frac{1}{3} - \frac{1}{\sqrt{3}}\varrho_\omega^{(8)} \right). \quad (27c)$$

Noting the difference between the definition of ϱ_ω for

neutrinos and antineutrinos [Eq. (13)], we have

$$n_{\bar{\nu}_1}(\omega) = n_\nu^{\text{tot}} f_\omega \left(\frac{1}{3} - \frac{1}{2}\varrho_\omega^{(3)} - \frac{1}{2\sqrt{3}}\varrho_\omega^{(8)} \right), \quad (28a)$$

$$n_{\bar{\nu}_2}(\omega) = n_\nu^{\text{tot}} f_\omega \left(\frac{1}{3} + \frac{1}{2}\varrho_\omega^{(3)} - \frac{1}{2\sqrt{3}}\varrho_\omega^{(8)} \right), \quad (28b)$$

$$n_{\bar{\nu}_3}(\omega) = n_\nu^{\text{tot}} f_\omega \left(\frac{1}{3} + \frac{1}{\sqrt{3}}\varrho_\omega^{(8)} \right). \quad (28c)$$

The relation between ω and the energy of a neutrino or antineutrino is described in Eq. (9).

One can define the cross and dot products of two 8-dimensional vectors \mathbf{A} and \mathbf{B} to be

$$\mathbf{A} \times \mathbf{B} \equiv -i \text{Tr}([\mathbf{A}, \mathbf{B}]\lambda_a) \hat{\mathbf{e}}_a = f_{abc} A^{(b)} B^{(c)} \hat{\mathbf{e}}_a, \quad (29a)$$

$$\mathbf{A} \cdot \mathbf{B} \equiv 2 \text{Tr}(\mathbf{A}\mathbf{B}) - \frac{2}{3} \text{Tr}(\mathbf{A}) \text{Tr}(\mathbf{B}) = A^{(a)} B^{(a)}, \quad (29b)$$

where $\hat{\mathbf{e}}_a$ is the a 'th unit vector in the 8-dimensional flavor space, and f_{abc} are the antisymmetric structure constants of $\text{SU}(3)$:

$$\left[\frac{\lambda_a}{2}, \frac{\lambda_b}{2} \right] = i f_{abc} \frac{\lambda_c}{2}. \quad (30)$$

The summation over Gell-Mann indices are implicitly assumed in the above equations when they appear twice in the subscripts or superscripts. Using Eqs. (15) and (29a) we can write the e.o.m. for flavor vector $\boldsymbol{\varrho}_\omega$ as

$$\frac{d}{dt} \boldsymbol{\varrho}_\omega = -\boldsymbol{\varrho}_\omega \times \mathbf{H}_\omega, \quad (31a)$$

$$= \boldsymbol{\varrho}_\omega \times \left(\omega \hat{\mathbf{e}}_3 + \frac{2\kappa}{\sqrt{3}} \hat{\mathbf{e}}_8 \right) - \mu \boldsymbol{\varrho}_\omega \times \int_{-\infty}^{\infty} d\omega' f_{\omega'} \boldsymbol{\varrho}_{\omega'}. \quad (31b)$$

The first term in Eq. (31b) corresponds the precession of $\boldsymbol{\varrho}_\omega$ around an “external field”, and the second term corresponds a “spin-spin anti-coupling” with strength μ .

Eq. (31a) makes it clear that the change in $\boldsymbol{\varrho}_\omega$ is orthogonal to $\boldsymbol{\varrho}_\omega$ itself, and, therefore, the magnitude of this quantity does not changed. We have

$$|\boldsymbol{\varrho}_\omega|^2 = \sum_a [\text{Tr}(\varrho_\omega \lambda_a)]^2 = \text{const.} \quad (32)$$

This is a natural result that also follows from the fact that Eqs. (4) and (7) maintain the coherence of $\rho_{\mathbf{p}}$ and $\bar{\rho}_{\mathbf{p}}$. Following Ref. [16] we define the effective energy of the system to be

$$\begin{aligned} \mathcal{E} \equiv & - \int_{-\infty}^{\infty} d\omega f_\omega \boldsymbol{\varrho}_\omega \cdot \left(\frac{\omega}{2} \hat{\mathbf{e}}_3 + \frac{\kappa}{\sqrt{3}} \hat{\mathbf{e}}_8 \right) \\ & + \frac{\mu}{4} \int_{-\infty}^{\infty} d\omega \int_{-\infty}^{\infty} d\omega' f_\omega f_{\omega'} \boldsymbol{\varrho}_\omega \cdot \boldsymbol{\varrho}_{\omega'}. \end{aligned} \quad (33)$$

Clearly the effective energy \mathcal{E} of the system is conserved if n_ν^{tot} is constant.

¹ Ref. [32] appears while this manuscript was in preparation. Ref. [32] has proposed a three-flavor version of the Bloch vector which is a generalization of the two-flavor polarization vector defined in Ref. [7]. The difference between the three-flavor Bloch vector and the flavor vector defined here is similar to that between the two-flavor polarization vector and the neutrino flavor isospin defined in Ref. [16]. In the flavor vector description, the directions of flavor vectors and flavor isospins for antineutrinos are intentionally reversed so that the e.o.m. for flavor vectors and flavor isospins (for both neutrinos and antineutrinos) can be written within a single expression. Likewise, the density matrix defined in Ref. [32] is different from the flavor density matrix in this paper by a sign for antineutrinos. This is of course a notation difference and does not affect the physical results.

Although flavor vector ϱ_ω seems to behave in a way similar to flavor isospin \mathbf{s}_ω in two-flavor mixing scenarios, there are fundamental differences between the 8-dimensional flavor vector space and the 3-dimensional flavor isospace. For example, two 8-dimensional vectors \mathbf{A} and \mathbf{B} are “perpendicular” or “parallel” to each other if $\mathbf{A} \cdot \mathbf{B} = 0$ or $\mathbf{A} \times \mathbf{B} = 0$, respectively. Because there are two linearly independent generators of $\text{SU}(3)$ that commute with each other, for any vector \mathbf{A} one can always find another vector \mathbf{A}' which is both “perpendicular” and “parallel” to \mathbf{A} . Consequently, generally speaking

$$\mathbf{B} \neq \mathbf{A} \frac{\mathbf{A} \cdot \mathbf{B}}{|\mathbf{A}|^2} \quad (34)$$

even if \mathbf{B} is “parallel” to \mathbf{A} .

The existence of two linearly independent and commuting generators of $\text{SU}(3)$ has another important consequence. Because $[\lambda_3, \lambda_8] = 0$, rotations around $\hat{\mathbf{e}}_3$ and $\hat{\mathbf{e}}_8$ can be viewed as independent. In particular, the first term in Eq. (31b) can be interpreted as simultaneous but independent precession of flavor vector ϱ_ω around $\hat{\mathbf{e}}_3$ and $\hat{\mathbf{e}}_8$ with generally different angular velocities.

Although the density matrix and flavor vector descriptions are equivalent, the rotation of a flavor vector in the 8-dimensional flavor space is not easily visualizable. Therefore, we will base our discussions mostly on the density matrix formalism with intermittent references to the flavor vector notation where it seems convenient.

C. Conserved “Lepton Numbers”

Multiplying Eq. (15) by f_ω and integrating it over ω we obtain the e.o.m. for ϱ_{tot} :

$$i\dot{\varrho}_{\text{tot}} = \frac{1}{2} \int_{-\infty}^{\infty} d\omega f_\omega \omega [\varrho_\omega, \lambda_3] + \frac{1}{\sqrt{3}} \int_{-\infty}^{\infty} d\omega f_\omega \kappa [\varrho_\omega, \lambda_8]. \quad (35)$$

Eq. (35) is not a closed equation from which we could solve for ϱ_{tot} . However, because λ_3 and λ_8 commute with each other, it is clear that the two “lepton numbers”

$$L_3 \equiv \varrho_{\text{tot}}^{(3)} = \int_{-\infty}^{\infty} d\omega f_\omega \text{Tr}(\varrho_\omega \lambda_3) \quad (36a)$$

and

$$L_8 \equiv \varrho_{\text{tot}}^{(8)} = \int_{-\infty}^{\infty} d\omega f_\omega \text{Tr}(\varrho_\omega \lambda_8) \quad (36b)$$

are constants of the motion. Because $\text{Tr}(\varrho_{\text{tot}})$ does not change with time, the lepton number (fraction) in each vacuum mass eigenstate is individually conserved.

D. Corotating Frame

In the density matrix description, changing from the static frame to a corotating frame corresponds to a trans-

formation

$$\varrho_\omega \rightarrow \tilde{\varrho}_\omega \equiv e^{i\mathbf{H}_{\text{cor}} t} \varrho_\omega e^{-i\mathbf{H}_{\text{cor}} t}, \quad (37)$$

where \mathbf{H}_{cor} is a 3×3 Hermitian matrix that is common to all neutrino modes and does not change with time. The flavor density matrix $\tilde{\varrho}_\omega$ in the corotating frame satisfies an e.o.m. similar to that in Eq. (15):

$$i\dot{\tilde{\varrho}}_\omega = [\tilde{\mathbf{H}}_\omega, \tilde{\varrho}_\omega], \quad (38)$$

where

$$\tilde{\mathbf{H}}_\omega \equiv e^{i\mathbf{H}_{\text{cor}} t} \mathbf{H}_\omega e^{-i\mathbf{H}_{\text{cor}} t} - \mathbf{H}_{\text{cor}} \quad (39)$$

is the Hamiltonian for neutrino mode ω in the corotating frame associated with \mathbf{H}_{cor} .

A very special set of corotating frames corresponds to simultaneous rotations around $\hat{\mathbf{e}}_3$ and $\hat{\mathbf{e}}_8$ with angular velocities Ω and $2K/\sqrt{3}$, respectively, and

$$\mathbf{H}_{\text{cor}} = -\Omega \frac{\lambda_3}{2} - K \frac{\lambda_8}{\sqrt{3}}. \quad (40)$$

Because $\mathbf{H}_\omega^{\text{vac}}$, λ_3 and λ_8 commute with each other, $\tilde{\mathbf{H}}_\omega$ in these special corotating frames takes the same form as \mathbf{H}_ω in Eq. (16) except for the replacements

$$\omega \rightarrow \omega - \Omega, \quad (41a)$$

$$\kappa \rightarrow \kappa - K, \quad (41b)$$

$$\varrho_{\text{tot}} \rightarrow \tilde{\varrho}_{\text{tot}} = e^{i\mathbf{H}_{\text{cor}} t} \varrho_{\text{tot}} e^{-i\mathbf{H}_{\text{cor}} t}. \quad (41c)$$

Also, because the occupation numbers of each vacuum eigenstate in a neutrino mode ω are determined only by $\varrho_\omega^{(3)}$ and $\varrho_\omega^{(8)}$, the probability for the neutrino mode to be in the i 'th vacuum mass eigenstate in these special corotating frames, $|\tilde{a}_{\nu_i}(\omega)|^2$, is the same as the probability for the neutrino mode to be in the same eigenstate in the static frame, $|a_{\nu_i}(\omega)|^2$. Therefore, lepton numbers L_3 and L_8 are not changed by the corotating-frame transformation either.

III. ADIABATIC/PRECESSION SOLUTION AND STEPWISE SPECTRAL SWAPPING

We now seek a natural extension to the adiabatic/precession solution presented in Ref. [25]. This solution, like the 2×2 case, will be essentially a quasi-static solution that, for given n_ν^{tot} , is the same as the “static” solution which satisfies the *precession ansatz*. There is a family of static solutions for each value of n_ν^{tot} . So long as n_ν^{tot} changes slowly, a particular solution in each family parametrized by n_ν^{tot} is uniquely determined by the initial conditions and by the *adiabatic ansatz*. This gives the adiabatic/precession solution. We will discuss the precession ansatz and three-flavor synchronization in Sec. III A. In Sec. III B we will discuss the adiabatic ansatz and outline a formal procedure for obtaining a three-flavor adiabatic/precession solution. In Sec. III C we will illustrate with a numerical example how stepwise spectral swapping arises from the three-flavor adiabatic/precession solution as $n_\nu^{\text{tot}} \rightarrow 0$.

A. The Precession Ansatz and Synchronization

The *precession ansatz* is that, for constant n_ν^{tot} , it is possible to find a Hermitian matrix

$$\mathbf{H}_{\text{cor}} = -\Omega_{\text{pr}} \frac{\lambda_3}{2} - K_{\text{pr}} \frac{\lambda_8}{\sqrt{3}} \quad (42)$$

such that the flavor density matrix $\tilde{\rho}_\omega$ is static in the corotating frame associated with \mathbf{H}_{cor} , i.e.

$$[\tilde{\mathbf{H}}_\omega, \tilde{\rho}_\omega] = 0. \quad (43)$$

From the arguments in Sec. II D, if the precession ansatz is satisfied, $|a_{\nu_i}(\omega)|^2$ does not change with time. In this sense, a solution that satisfies the precession ansatz is “static”.

When the adiabatic ansatz is satisfied, each flavor vector $\boldsymbol{\rho}_\omega$ will precess uniformly around $\hat{\mathbf{e}}_3$ and $\hat{\mathbf{e}}_8$. In other words, the system is in a state that is symmetric about $\hat{\mathbf{e}}_3$ and $\hat{\mathbf{e}}_8$. Because the e.o.m. for $\boldsymbol{\rho}_\omega$ [Eqs. (31)] possess the same symmetry around the $\hat{\mathbf{e}}_3$ and $\hat{\mathbf{e}}_8$ axes, we expect “static” precession solutions to exist for constant n_ν^{tot} with appropriate initial conditions. In particular, this symmetry obtains approximately in dense neutrino gases where

$$\mu = \sqrt{2} G_F n_\nu^{\text{tot}} \gg |\kappa| \gg |\omega| \quad (44)$$

for most neutrino modes. This conclusion can be shown as follows.

When Eq. (44) is satisfied, the conserved effective energy of the system is [Eq. (33)]

$$\mathcal{E} \simeq \frac{\mu}{4} |\boldsymbol{\rho}_{\text{tot}}|^2 \quad (45)$$

and, therefore,

$$|\boldsymbol{\rho}_{\text{tot}}| \simeq \text{const.} \quad (46)$$

Because the two lepton numbers $L_3 = \rho_{\text{tot}}^{(3)}$ and $L_8 = \rho_{\text{tot}}^{(8)}$ are conserved (Sec. II C), the total flavor vector $\boldsymbol{\rho}_{\text{tot}}$ must precess simultaneously around $\hat{\mathbf{e}}_3$ and $\hat{\mathbf{e}}_8$ according to

$$\frac{d}{dt} \boldsymbol{\rho}_{\text{tot}} \simeq \boldsymbol{\rho}_{\text{tot}} \times \left(\Omega_{\text{pr}}^\infty \hat{\mathbf{e}}_3 + \frac{2K_{\text{pr}}^\infty}{\sqrt{3}} \hat{\mathbf{e}}_8 \right). \quad (47)$$

Also in this limit, Eq. (31) becomes

$$\frac{d}{dt} \boldsymbol{\rho}_\omega \simeq -\mu \boldsymbol{\rho}_\omega \times \boldsymbol{\rho}_{\text{tot}}. \quad (48)$$

Eqs. (47) and (48) suggests a simple geometric picture for the flavor evolution in dense neutrino gases. On short time scales ($\Delta t \sim \mu^{-1}$), each flavor vector $\boldsymbol{\rho}_\omega$ precess rapidly around the total flavor vector $\boldsymbol{\rho}_{\text{tot}}$. On large time scales ($\Delta t \sim |\Omega_{\text{pr}}^\infty|^{-1}, |K_{\text{pr}}^\infty|^{-1}$), all flavor vectors precess slowly around $\hat{\mathbf{e}}_3$ and $\hat{\mathbf{e}}_8$ with angular velocities $\Omega_{\text{pr}}^\infty$ and $2K_{\text{pr}}^\infty/\sqrt{3}$, respectively. This is analogous to the synchronization phenomenon in two-flavor mixing scenarios [12].

B. The Adiabatic Ansatz and Adiabatic/Precession Solutions

When the precession ansatz in Eq. (43) is satisfied, it is possible to find a unitary matrix \mathbf{X}_ω that simultaneously diagonalizes both $\tilde{\mathbf{H}}_\omega$ and $\tilde{\rho}_\omega$:

$$\mathbf{X}_\omega \tilde{\mathbf{H}}_\omega \mathbf{X}_\omega^\dagger = \text{diag}(\tilde{\omega}_L, \tilde{\omega}_M, \tilde{\omega}_H), \quad (49a)$$

$$\mathbf{X}_\omega \tilde{\rho}_\omega \mathbf{X}_\omega^\dagger = \pm \text{diag}(|a_{\tilde{\nu}_L}|^2, |a_{\tilde{\nu}_M}|^2, |a_{\tilde{\nu}_H}|^2), \quad (49b)$$

where $\tilde{\omega}_L < \tilde{\omega}_M < \tilde{\omega}_H$ are the eigenvalues corresponding to the eigenstates of $\tilde{\mathbf{H}}_\omega$, $|\tilde{\nu}_L(\omega)\rangle$, $|\tilde{\nu}_M(\omega)\rangle$ and $|\tilde{\nu}_H(\omega)\rangle$. In Eq. (49b) the plus (minus) sign is for neutrinos (antineutrinos). The *adiabatic ansatz* is simply that

$$|a_{\tilde{\nu}_l}(\omega)|^2 = \text{const.} \quad (l = L, M, H) \quad (50)$$

as n_ν^{tot} slowly varies with time.

As discussed in Ref. [27], this “adiabaticity” criterion connects neutrino systems in different corotating frames at different values of n_ν^{tot} . Note that this adiabaticity criterion is different from the meaning of adiabaticity usually adopted in the literature, e.g., when discussing the MSW mechanism, which is always based on the static frame. Following Ref. [25], we argue here that the adiabatic ansatz can be satisfied if, for each neutrino mode ω , $\tilde{\mathbf{H}}_\omega$ rotates at a speed much slower than precession rate of $\tilde{\rho}_\omega$ around $\tilde{\mathbf{H}}_\omega$, i.e.

$$\gamma \equiv \frac{|\tilde{\mathbf{H}}_\omega \times d\tilde{\mathbf{H}}_\omega/dt|}{|\tilde{\mathbf{H}}_\omega|^3} \ll 1. \quad (51)$$

The adiabatic/precession solution can be obtained formally by employing the following procedure:

1. At any n_ν^{tot} find for each neutrino mode ω a unitary matrix \mathbf{X}_ω that diagonalizes $\tilde{\mathbf{H}}_\omega$. Matrix \mathbf{X}_ω is expressed as a function of $(\tilde{\rho}_{\text{tot}}, \Omega_{\text{pr}}, K_{\text{pr}})$.
2. For given initial values of $|a_{\tilde{\nu}_l}(\omega)|^2$, find $\tilde{\rho}_\omega = \pm \mathbf{X}_\omega^\dagger \text{diag}(|a_{\tilde{\nu}_L}|^2, |a_{\tilde{\nu}_M}|^2, |a_{\tilde{\nu}_H}|^2) \mathbf{X}_\omega$ as a function of $(\tilde{\rho}_{\text{tot}}, \Omega_{\text{pr}}, K_{\text{pr}})$.
3. For given initial lepton numbers L_3 and L_8 find $\tilde{\rho}_{\text{tot}}^{(3)} = L_3$ and $\tilde{\rho}_{\text{tot}}^{(8)} = L_8$. From the definition $\tilde{\rho}_{\text{tot}} = \int_{-\infty}^{\infty} d\omega f_\omega \tilde{\rho}_\omega(\tilde{\rho}_{\text{tot}}, \Omega_{\text{pr}}, K_{\text{pr}})$, solve for the precession angular velocities Ω_{pr} and K_{pr} and the remaining components of $\tilde{\rho}_{\text{tot}}$.
4. Find $\tilde{\rho}_\omega$ for each neutrino mode ω using the expression $\tilde{\rho}_\omega(\tilde{\rho}_{\text{tot}}, \Omega_{\text{pr}}, K_{\text{pr}})$ obtained in step 2.

We note that the above procedure actually gives a set of equivalent solutions. This is because the precession solution is symmetric around $\hat{\mathbf{e}}_3$ and $\hat{\mathbf{e}}_8$. If $(\tilde{\rho}_{\text{tot}}, \Omega_{\text{pr}}, K_{\text{pr}})$ is a solution, $(\tilde{\rho}'_{\text{tot}}, \Omega_{\text{pr}}, K_{\text{pr}})$ is also a solution, where $\tilde{\rho}'_{\text{tot}}$ is related to $\tilde{\rho}_{\text{tot}}$ by two arbitrary phases ϕ_3 and ϕ_8 :

$$\tilde{\rho}'_{\text{tot}} = \exp\left(-i\phi_3 \frac{\lambda_3}{2} - i\phi_8 \frac{\lambda_8}{2}\right) \tilde{\rho}_{\text{tot}} \exp\left(i\phi_3 \frac{\lambda_3}{2} + i\phi_8 \frac{\lambda_8}{2}\right). \quad (52)$$

One can fix these two phases by, e.g., choosing $\tilde{\rho}_{\text{tot}}^{(2)} = \tilde{\rho}_{\text{tot}}^{(7)} = 0$.

C. Stepwise Spectral Swapping

Neutrino flavor mixing becomes very simple in the adiabatic/precession solution presented in Sec. IIIB when $n_\nu^{\text{tot}} \rightarrow 0$. In this limit \tilde{H}_ω is diagonal in the vacuum mass basis:

$$\tilde{H}_\omega|_{n_\nu^{\text{tot}} \rightarrow 0} = \text{diag}(\tilde{\omega}_1, \tilde{\omega}_2, \tilde{\omega}_3)_{n_\nu^{\text{tot}} \rightarrow 0}, \quad (53)$$

where

$$\tilde{\omega}_1|_{n_\nu^{\text{tot}} \rightarrow 0} = -\frac{1}{2}(\omega - \Omega_{\text{pr}}^0) - \frac{1}{3}(\kappa - K_{\text{pr}}^0), \quad (54a)$$

$$\tilde{\omega}_2|_{n_\nu^{\text{tot}} \rightarrow 0} = \frac{1}{2}(\omega - \Omega_{\text{pr}}^0) - \frac{1}{3}(\kappa - K_{\text{pr}}^0), \quad (54b)$$

$$\tilde{\omega}_3|_{n_\nu^{\text{tot}} \rightarrow 0} = \frac{2}{3}(\kappa - K_{\text{pr}}^0), \quad (54c)$$

with Ω_{pr}^0 and K_{pr}^0 being the collective precession angular velocities as $n_\nu^{\text{tot}} \rightarrow 0$. Eq. (53) shows that $\tilde{H}_\omega|_{n_\nu^{\text{tot}} \rightarrow 0}$ has 3 critical values of ω at which any two of its eigenvalues are equal. These critical values are

$$\omega_1^s = \Omega_{\text{pr}}^0, \quad (55a)$$

$$\omega_2^s = \frac{\Delta m_{21}^2}{\Delta m_{31}^2} \left(K_{\text{pr}}^0 + \frac{1}{2} \Omega_{\text{pr}}^0 \right), \quad (55b)$$

$$\omega_3^s = \frac{\Delta m_{21}^2}{\Delta m_{32}^2} \left(K_{\text{pr}}^0 - \frac{1}{2} \Omega_{\text{pr}}^0 \right). \quad (55c)$$

In practice, however, two of the critical points are usually indistinguishable

$$\omega_1^s = \omega_\odot^s \equiv \Omega_{\text{pr}}^0, \quad (56a)$$

$$\omega_2^s \simeq \omega_3^s \simeq \omega_{\text{atm}}^s \equiv \pm \frac{\Delta m_\odot^2}{\Delta m_{\text{atm}}^2} K_{\text{pr}}^0, \quad (56b)$$

because $\Delta m_{\text{atm}}^2 \gg \Delta m_\odot^2$ and, therefore, $|K_{\text{pr}}^0| \gg |\Omega_{\text{pr}}^0|$. In Eq. (56b) the positive (negative) sign is for the normal (inverted) neutrino mass hierarchy. A critical value ω^s corresponds to the energy where “stepwise spectral swapping” or a “spectral split” occurs. If $\omega^s > 0$, the spectral swap occurs at neutrino energy

$$E^s \simeq \frac{\Delta m_\odot^2}{2|\omega^s|} \quad (57)$$

in the neutrino sector. If $\omega^s < 0$, the swap is located in the antineutrino sector at energy E^s .

We can illustrate stepwise spectral swapping by using the following test example. We assume a bare, hot, spherical neutron-star that isotropically emits neutrinos directly into the vacuum from its infinitely thin neutrino sphere. We adopt the single-angle approximation and take the radius of the neutrino sphere to be $R_\nu = 30$ km, and the luminosity for each neutrino species to be $L_\nu = 10^{52}$ erg/s. We take the energy spectra of neutrinos to be of the Fermi-Dirac form:

$$f_\nu(E) = \frac{1}{T_\nu^3 F_2(\eta_\nu)} \frac{E^2}{\exp(E/T_\nu - \eta_\nu) + 1}, \quad (58)$$

where

$$F_k(\eta) = \int_0^\infty \frac{x^k dx}{\exp(x - \eta) + 1}. \quad (59)$$

We take degeneracy parameters to be the same for all neutrino species, $\eta_\nu = 3$, and we choose T_ν to be such that the average energies for various neutrino species are $\langle E_{\nu_e} \rangle = 11$ MeV, $\langle E_{\bar{\nu}_e} \rangle = 16$ MeV and $\langle E_{\nu_\mu} \rangle = \langle E_{\bar{\nu}_\mu} \rangle = \langle E_{\nu_\tau} \rangle = \langle E_{\bar{\nu}_\tau} \rangle = 25$ MeV, respectively. For the neutrino mixing parameters (see, e.g., Ref. [33] for our conventions) we take $\theta_{12} = 0.6$, $\theta_{13} = 0.1$, $\theta_{23} = \pi/4$, $\delta = 0$, $\Delta m_{21}^2 = 8 \times 10^{-5} \text{ eV}^2$ and $\Delta m_{32}^2 = -3 \times 10^{-3} \text{ eV}^2$ (inverted neutrino mass hierarchy).

We define $P(\nu_\alpha \rightarrow \nu_i)$ and $P(\bar{\nu}_\alpha \rightarrow \bar{\nu}_i)$ as the probabilities for neutrinos and antineutrinos that are initially in pure α flavor state at the neutrino sphere to end up in the i 'th vacuum mass eigenstate as $n_\nu^{\text{tot}} \rightarrow 0$. In Fig. 1 we show neutrino conversion probabilities $P(\nu_\alpha \rightarrow \nu_i)$ and $P(\bar{\nu}_\alpha \rightarrow \bar{\nu}_i)$ as functions of neutrino energies in our test example. We observe that while $P(\nu_\alpha \rightarrow \nu_i)$ shows two swaps at $E_\odot^s \simeq 5.2$ MeV and $E_{\text{atm}}^s \simeq 8.4$ MeV, respectively, $P(\bar{\nu}_\alpha \rightarrow \bar{\nu}_i)$ shows no swap at all. This phenomenon can be explained using the adiabatic/precession solution discussed above.

TABLE I: The correspondence between neutrino states $|\tilde{\nu}_l(\omega)\rangle$ and $|\nu_\alpha\rangle$ or $|\bar{\nu}_\alpha\rangle$ at $r = R_\nu$ for the inverted neutrino mass hierarchy case with mixing angles $\theta_{13} \simeq 0$ and $\theta_{23} \simeq \pi/4$.

	$\omega < 0$	$0 < \omega < \omega_{\text{atm}}^{\text{sync}}$	$\omega > \omega_{\text{atm}}^{\text{sync}}$
$ \tilde{\nu}_L(\omega)\rangle$	$\frac{1}{\sqrt{2}}(\bar{\nu}_\mu\rangle - \bar{\nu}_\tau\rangle)$	$\frac{1}{\sqrt{2}}(\nu_\mu\rangle - \nu_\tau\rangle)$	$\frac{1}{\sqrt{2}}(\nu_\mu\rangle + \nu_\tau\rangle)$
$ \tilde{\nu}_M(\omega)\rangle$	$\frac{1}{\sqrt{2}}(\bar{\nu}_\mu\rangle + \bar{\nu}_\tau\rangle)$	$\frac{1}{\sqrt{2}}(\nu_\mu\rangle + \nu_\tau\rangle)$	$\frac{1}{\sqrt{2}}(\nu_\mu\rangle - \nu_\tau\rangle)$
$ \tilde{\nu}_H(\omega)\rangle$	$ \bar{\nu}_e\rangle$	$ \nu_e\rangle$	$ \nu_e\rangle$

TABLE II: The correspondence between neutrino states $|\tilde{\nu}_l(\omega)\rangle$ and $|\nu_i\rangle$ or $|\bar{\nu}_i\rangle$ as $n_\nu^{\text{tot}} \rightarrow 0$ for the inverted mass hierarchy case and for swap points with hierarchy $\omega_\odot^s > \omega_{\text{atm}}^s > 0$.

	$\omega < 0$	$0 < \omega < \omega_{\text{atm}}^s$	$\omega_{\text{atm}}^s < \omega < \omega_\odot^s$	$\omega > \omega_\odot^s$
$ \tilde{\nu}_L(\omega)\rangle$	$ \bar{\nu}_2\rangle$	$ \nu_2\rangle$	$ \nu_3\rangle$	$ \nu_3\rangle$
$ \tilde{\nu}_M(\omega)\rangle$	$ \bar{\nu}_1\rangle$	$ \nu_1\rangle$	$ \nu_2\rangle$	$ \nu_1\rangle$
$ \tilde{\nu}_H(\omega)\rangle$	$ \bar{\nu}_3\rangle$	$ \nu_3\rangle$	$ \nu_1\rangle$	$ \nu_2\rangle$

TABLE III: Nonzero neutrino conversion probabilities $P(\nu_\alpha \rightarrow \nu_i)$ and $P(\bar{\nu}_\alpha \rightarrow \bar{\nu}_i)$ based on Tables I and II and the adiabaticity ansatz in Eq. (66).

energy range	nonzero conversion probabilities
any $E_{\bar{\nu}}$	$P(\bar{\nu}_e \rightarrow \bar{\nu}_3) = 2P(\bar{\nu}_{\mu,\tau} \rightarrow \bar{\nu}_{1,2}) = 1$
$E_\nu > E_{\text{atm}}^s$	$P(\nu_e \rightarrow \nu_3) = 2P(\nu_{\mu,\tau} \rightarrow \nu_{1,2}) = 1$
$E_\odot^s < E_\nu < E_{\text{atm}}^s$	$P(\nu_e \rightarrow \nu_1) = 2P(\nu_{\mu,\tau} \rightarrow \nu_{2,3}) = 1$
$E_\nu < E_\odot^s$	$P(\nu_e \rightarrow \nu_2) = 2P(\nu_{\mu,\tau} \rightarrow \nu_{1,3}) = 1$

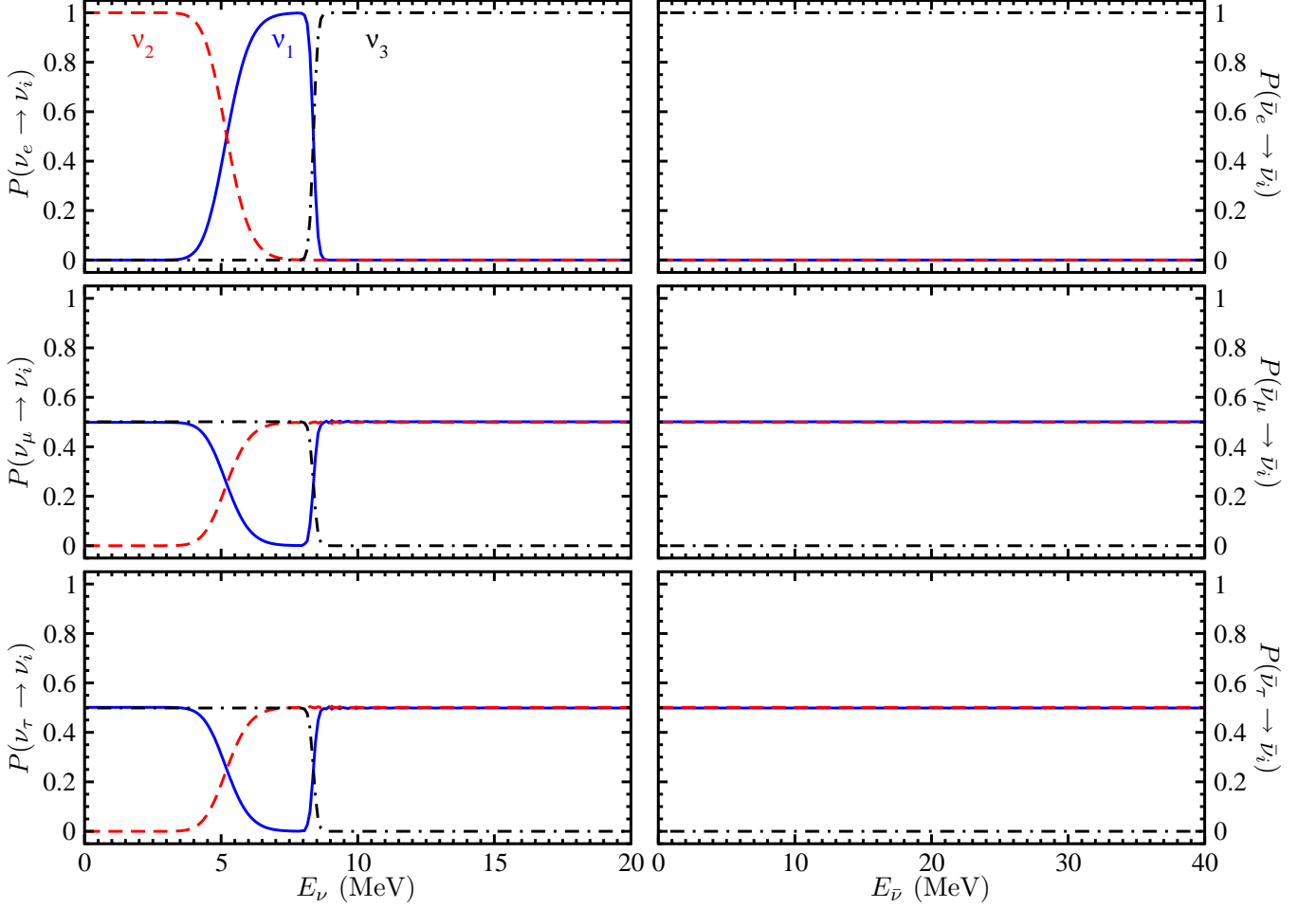


FIG. 1: (Color online) Conversion probabilities $P(\nu_\alpha \rightarrow \nu_i)$ (left panels) and $P(\bar{\nu}_\alpha \rightarrow \bar{\nu}_i)$ (right panels) as functions of neutrino and antineutrino energies E_ν and $E_{\bar{\nu}}$, respectively, in the bare, hot neutron star example. The top, middle and bottom panels are for neutrinos that are initially in pure e , μ and τ flavors, respectively. The solid, dashed and dot-dashed lines are for neutrinos that end up in the 1st, 2nd and 3rd vacuum mass eigenstates, respectively, when $n_\nu^{\text{tot}} \rightarrow 0$.

Assuming that the precession ansatz in Eq. (43) is satisfied, we can diagonalize the Hamiltonian $\tilde{H}_\omega|_{r=R_\nu}$ in the corotating frame in which all flavor vectors are static. We denote $\tilde{\omega}_L < \tilde{\omega}_M < \tilde{\omega}_H$ as eigenvalues corresponding to the eigenstates $|\tilde{\nu}_L\rangle$, $|\tilde{\nu}_M\rangle$ and $|\tilde{\nu}_H\rangle$ of $\tilde{H}_\omega|_{r=R_\nu}$, respectively. Because n_ν^{tot} is very large at the neutrino sphere, we have

$$\sqrt{2}G_F(n_{\nu_e} - n_{\bar{\nu}_e}) \gg |\omega - \Omega_{\text{pr}}^\infty|, |\kappa - K_{\text{pr}}^\infty| \quad (60)$$

for most neutrino modes. Therefore,

$$|\tilde{\nu}_H(\omega)\rangle_{r=R_\nu} \simeq \begin{cases} |\nu_e\rangle & \text{if } \omega > 0, \\ |\bar{\nu}_e\rangle & \text{if } \omega < 0. \end{cases} \quad (61)$$

We note that Ω_{pr} and K_{pr} are essentially a kind of average of ω and κ in the system. In our example, neutrinos (instead of antineutrinos) are the dominant species and the neutrino mass hierarchy is inverted. So we expect

$\Omega_{\text{pr}} > 0 > K_{\text{pr}}$ at any value of n_ν^{tot} . We can diagonalize the $\mu\tau$ -submatrix of $\tilde{H}_\omega^{\text{vac}}$ in the flavor basis and obtain

$$|\tilde{\nu}_L(\omega)\rangle_{r=R_\nu} \simeq \frac{1}{\sqrt{2}}(|\bar{\nu}_\mu\rangle - |\bar{\nu}_\tau\rangle), \quad (62a)$$

$$|\tilde{\nu}_M(\omega)\rangle_{r=R_\nu} \simeq \frac{1}{\sqrt{2}}(|\bar{\nu}_\mu\rangle + |\bar{\nu}_\tau\rangle), \quad (62b)$$

if $\omega < 0$, and

$$|\tilde{\nu}_L(\omega)\rangle_{r=R_\nu} \simeq \frac{1}{\sqrt{2}}(|\nu_\mu\rangle \mp |\nu_\tau\rangle), \quad (63a)$$

$$|\tilde{\nu}_M(\omega)\rangle_{r=R_\nu} \simeq \frac{1}{\sqrt{2}}(|\nu_\mu\rangle \pm |\nu_\tau\rangle), \quad (63b)$$

if $\omega > 0$. In Eq. (63), the upper and lower signs are for the cases where ω is smaller or larger than

$$\omega_{\text{atm}}^{\text{sync}} = -K_{\text{pr}}^\infty \frac{\Delta m_{\odot}^2}{\Delta m_{\text{atm}}^2}, \quad (64)$$

respectively. Here $|\tilde{\nu}_L(\omega)\rangle_{r=R_\nu}$ and $|\tilde{\nu}_M(\omega)\rangle_{r=R_\nu}$ are “equal mixes” of $|\nu_\mu\rangle$ and $|\nu_\tau\rangle$ or $|\bar{\nu}_\mu\rangle$ and $|\bar{\nu}_\tau\rangle$. These results are summarized in Table I.

Far away from the neutron star where $n_\nu^{\text{tot}} \rightarrow 0$, we obtain $|\tilde{\nu}_l\rangle_{n_\nu^{\text{tot}} \rightarrow 0}$ using Eqs. (53) and (54). For $\omega < 0$ (antineutrinos) we have

$$|\tilde{\nu}_L(\omega)\rangle_{n_\nu^{\text{tot}} \rightarrow 0} = |\bar{\nu}_2\rangle, \quad (65a)$$

$$|\tilde{\nu}_M(\omega)\rangle_{n_\nu^{\text{tot}} \rightarrow 0} = |\bar{\nu}_1\rangle, \quad (65b)$$

$$|\tilde{\nu}_H(\omega)\rangle_{n_\nu^{\text{tot}} \rightarrow 0} = |\bar{\nu}_3\rangle. \quad (65c)$$

Assuming that $\omega_\odot^s > \omega_{\text{atm}}^s > 0$, we summarize the correspondence between $|\tilde{\nu}_l(\omega)\rangle$ and $|\nu_i\rangle$ for $n_\nu^{\text{tot}} \rightarrow 0$ in Table II.

If the adiabatic ansatz in Eq. (50) is satisfied, we have

$$|a_{\tilde{\nu}_l}(\omega)|_{r=R_\nu}^2 = |a_{\tilde{\nu}_l}(\omega)|_{n_\nu^{\text{tot}} \rightarrow 0}^2 \quad (66)$$

for each neutrino mode ω . Using Eq. (66) and Tables I and II, we can obtain the neutrino conversion probabilities $P(\nu_\alpha \rightarrow \nu_i)$ and $P(\bar{\nu}_\alpha \rightarrow \bar{\nu}_i)$ for each neutrino mode ω . In Table III we summarize the values of nonzero neutrino conversion probability when the flavor evolution of the neutrino gas follows the adiabatic/precession solution. The results in Table III and Fig. 1 are in good agreement. The neutrino spectral swapping feature in Fig. 1 indeed can be explained by the adiabatic/precession solution.

As in two-flavor scenarios, the swapping energies E_\odot^s and E_{atm}^s can be obtained by using the conservation of lepton numbers and by assuming that the spectral swaps are infinitely sharp in energy. From conservation of $L_8 = \varrho_{\text{tot}}^{(8)}$ we have

$$\sqrt{3}L_8 \stackrel{r=R_\nu}{\simeq} \int_0^\infty dE (\tilde{f}_{\nu_e} - \tilde{f}_{\bar{\nu}_e}), \quad (67a)$$

$$\stackrel{n_\nu^{\text{tot}} \rightarrow 0}{\simeq} \int_0^{E_{\text{atm}}^s} dE (\tilde{f}_{\nu_e} - \tilde{f}_{\nu_x}) + \int_{E_{\text{atm}}^s}^\infty dE (2\tilde{f}_{\nu_x} - 2\tilde{f}_{\nu_e}) - \int_0^\infty dE (2\tilde{f}_{\bar{\nu}_x} - 2\tilde{f}_{\bar{\nu}_e}), \quad (67b)$$

where $\tilde{f}_\nu(E)$ is a distribution function which satisfies

$$\tilde{f}_\nu(E) \propto f_\nu(E) \quad (68)$$

with normalization condition

$$\sum_\nu \int_0^\infty dE \tilde{f}_\nu(E) = 1, \quad (69)$$

and

$$\tilde{f}_{\nu_x} = \tilde{f}_{\nu_\mu} = \tilde{f}_{\bar{\nu}_\mu} = \tilde{f}_{\nu_\tau} = \tilde{f}_{\bar{\nu}_\tau}. \quad (70)$$

From Eq. (67) we can determine that $E_{\text{atm}}^s \simeq 8.4$ MeV. We also can obtain E_\odot^s from the conservation of $L_3 = \varrho_{\text{tot}}^{(3)}$:

$$L_3 \stackrel{r=R_\nu}{\simeq} \int_0^\infty dE \cos 2\theta_{12} (\tilde{f}_{\nu_e} - \tilde{f}_{\bar{\nu}_e}), \quad (71a)$$

$$\stackrel{n_\nu^{\text{tot}} \rightarrow 0}{\simeq} \int_0^{E_\odot^s} dE (\tilde{f}_{\nu_x} - \tilde{f}_{\nu_e}) + \int_{E_\odot^s}^{E_{\text{atm}}^s} dE (\tilde{f}_{\nu_e} - \tilde{f}_{\nu_x}). \quad (71b)$$

This implies $E_\odot^s \simeq 5.3$ MeV. The values for E_{atm}^s and E_\odot^s derived from the adiabatic/precession solution are also in good agreement with the numerical results shown in Fig. 1.

We note that, in this numerical example, neutrinos of the μ and τ flavors are equally mixed and have identical energy spectra initially. In this particular case, the

two-flavor approximation with effective mixing parameters $\Delta m^2 \simeq -\Delta m_{\text{atm}}^2$ and $\theta \simeq \theta_{13}$ produce a similar spectral swapping feature around $E_{2 \times 2}^s = E_{\text{atm}}^s$. In the two-flavor mixing scenario, the value for $E_{2 \times 2}^s$ is also determined by the conservation of a lepton number

$$L_{2 \times 2} \stackrel{r=R_\nu}{\simeq} I_1 + I_2, \quad (72a)$$

$$\stackrel{n_\nu^{\text{tot}} \rightarrow 0}{\simeq} I_1 - I_2, \quad (72b)$$

where

$$I_1 = \int_0^{E_{2 \times 2}^s} dE (\tilde{f}_{\nu_e} - \tilde{f}_{\nu_x}), \quad (73a)$$

$$I_2 = \int_{E_{2 \times 2}^s}^\infty dE (\tilde{f}_{\nu_e} - \tilde{f}_{\nu_x}) - \int_0^\infty dE (\tilde{f}_{\bar{\nu}_e} - \tilde{f}_{\bar{\nu}_x}). \quad (73b)$$

From Eq. (72) it is easy to see that the integral $I_2 = 0$. Comparing Eqs. (67) and (72), we see that a solution for $E_{2 \times 2}^s$ in Eq. (72) is a solution for $E_{\text{atm}}^s = E_{2 \times 2}^s$ in Eq. (67). Therefore, the two-flavor spectral swap phenomenon is completely consistent with the three-flavor spectral swap phenomenon at the atmospheric mass-squared-difference scale.

We also note that, in this example, there would exist only one spectral swap at energy $E_\nu \simeq E_{\text{atm}}^s$ if we had chosen the other hierarchy for swap points, i.e. $\omega_{\text{atm}}^s > \omega_\odot^s > 0$. It is generally not possible for a single spectral swap to satisfy the conservation of both lepton

numbers and, therefore, this hierarchy for swap points is not physical.

The example given here can be generalized into a generic procedure to predict neutrino spectral swaps:

1. Diagonalize \tilde{H}_ω when n_ν^{tot} is large, and find the correspondence between $|\tilde{\nu}_l(\omega)\rangle$ and $|\nu_\alpha\rangle$ or $|\bar{\nu}_\alpha\rangle$ as was done in Table I.
2. Estimate the approximate locations of the swap points as $n_\nu^{\text{tot}} \rightarrow 0$. The swap points are expected to be in the neutrino sector if the system is dominated by neutrinos instead of antineutrinos. Pick a hierarchy for swap points, i.e., whether $E_{\text{atm}}^s > E_\odot^s$ or $E_{\text{atm}}^s < E_\odot^s$.
3. Obtain from Eq. (54) the correspondence between $|\tilde{\nu}_l(\omega)\rangle$ and $|\nu_i\rangle$ or $|\bar{\nu}_i\rangle$ for $n_\nu^{\text{tot}} \rightarrow 0$, as was done in Table II.
4. Use the results in step 1 and 3 and the adiabatic ansatz in Eq. (66) to find neutrino conversion probabilities $P(\nu_\alpha \rightarrow \nu_i)$ and $P(\bar{\nu}_\alpha \rightarrow \bar{\nu}_i)$, as was done in Table III.
5. Find lepton numbers L_3 and L_8 as $n_\nu^{\text{tot}} \rightarrow 0$. These will be functions of E_\odot^s and E_{atm}^s when the initial energy spectra $f_\nu(E)$ and the results in step 4 are used.
6. Solve for E_\odot^s and E_{atm}^s by using lepton number conservation $L_3|_{t=0} = L_3|_{n_\nu^{\text{tot}} \rightarrow 0}(E_\odot^s, E_{\text{atm}}^s)$ and $L_8|_{t=0} = L_8|_{n_\nu^{\text{tot}} \rightarrow 0}(E_\odot^s, E_{\text{atm}}^s)$. If no consistent solution can be found, pick the other hierarchy for swap points E_\odot^s and E_{atm}^s in step 2 and repeat steps 3–6.

IV. ADIABATIC/PRECESSION SOLUTIONS IN A DOMINANT MATTER BACKGROUND

A. Effects of Neutrino-Electron Forward Scattering

In the presence of ordinary matter, Eq. (15) is still valid except that the Hamiltonian for neutrino mode ω

becomes

$$H_\omega = H_\omega^{\text{vac}} + H^{\text{matt}} + \mu \varrho_{\text{tot}}, \quad (74)$$

where H^{matt} is the Hamiltonian contribution arising from neutrino-electron forward scattering. In general this term will give different refractive indices for $\nu_e/\bar{\nu}_e$ and $\nu_{\mu,\tau}/\bar{\nu}_{\mu,\tau}$ [1, 2, 3]. Ignoring the trace term, in the flavor basis we can write

$$H^{\text{matt}} = \sqrt{2}G_F n_b \text{diag}(Y_e, 0, 0), \quad (75)$$

where n_b is the number density of baryons, and Y_e is the electron fraction. MSW resonances can occur if $n_e = n_b Y_e$ is small and comparable to $|\omega|/\sqrt{2}G_F$ or $|\kappa|/\sqrt{2}G_F$. In this section, however, we will assume n_e to be constant and very large for most neutrino modes:

$$n_e \gg \frac{|\kappa|}{\sqrt{2}G_F}. \quad (76)$$

Because H^{matt} is independent of ω , it vanishes in the corotating frame picked out by

$$H_{\text{cor}} = H^{\text{matt}}. \quad (77)$$

In this corotating frame, the vacuum Hamiltonian for neutrino mode ω becomes

$$\tilde{H}_\omega^{\text{vac}} \simeq \frac{\omega}{\Delta m_{21}^2} \begin{pmatrix} m_1^2 c_{12}^2 + m_2^2 s_{12}^2 & \tilde{h}_{12}(t) & \tilde{h}_{13}(t) \\ \tilde{h}_{12}^*(t) & \frac{1}{2}(m_3^2 + m_1^2 s_{12}^2 + m_2^2 c_{12}^2) & \frac{1}{2}(m_3^2 - m_1^2 s_{12}^2 - m_2^2 c_{12}^2) \\ \tilde{h}_{13}^*(t) & \frac{1}{2}(m_3^2 - m_1^2 s_{12}^2 - m_2^2 c_{12}^2) & \frac{1}{2}(m_3^2 + m_1^2 s_{12}^2 + m_2^2 c_{12}^2) \end{pmatrix} \quad (78)$$

in the flavor basis, where $c_{ij} = \cos \theta_{ij}$, $s_{ij} = \sin \theta_{ij}$, and $\tilde{h}_{12}(t)$ and $\tilde{h}_{13}(t)$ are functions that oscillate with angular frequency $\sqrt{2}G_F n_e$. In deriving Eq. (78) we have taken

$\theta_{13} \simeq 0$ and $\theta_{23} \simeq \pi/4$. Because

$$\sqrt{2}G_F n_e \gg |\tilde{h}_{12}(t)|, |\tilde{h}_{13}(t)|, \quad (79)$$

we expect $\tilde{h}_{12}(t)$ and $\tilde{h}_{13}(t)$ to average to 0 and, therefore,

to have little effect on neutrino flavor evolution.

Setting $\tilde{h}_{12}(t)$ and $\tilde{h}_{13}(t)$ to 0, we can diagonalize $\tilde{H}_\omega^{\text{vac}}$:

$$\tilde{H}_\omega^{\text{vac}} \rightarrow \frac{\omega}{\Delta m_{21}^2} \text{diag}(m_1'^2, m_2'^2, m_3'^2), \quad (80)$$

where

$$m_1'^2 \simeq c_{12}^2 m_1^2 + s_{12}^2 m_2^2, \quad (81a)$$

$$m_2'^2 \simeq s_{12}^2 m_1^2 + c_{12}^2 m_2^2, \quad (81b)$$

$$m_3'^2 \simeq m_3^2 \quad (81c)$$

are the effective mass-squared values for neutrino states

$$|\nu_1'\rangle \simeq |\nu_e\rangle, \quad (82a)$$

$$|\nu_2'\rangle \simeq \frac{1}{\sqrt{2}}(|\nu_\mu\rangle - |\nu_\tau\rangle), \quad (82b)$$

$$|\nu_3'\rangle \simeq \frac{1}{\sqrt{2}}(|\nu_\mu\rangle + |\nu_\tau\rangle). \quad (82c)$$

We note that the flavor density matrix $\tilde{\varrho}_\omega$ in the corotating frame associated with $H_{\text{cor}} = H^{\text{matt}}$ obeys an e.o.m. similar to that obeyed by ϱ_ω in vacuum [Eq. (15)], except for small perturbations occurring on very short time scales ($\Delta t \sim G_F^{-1} n_e^{-1}$). The only difference is that the presence of a large net electron background breaks the “degeneracy” between $\nu_e/\bar{\nu}_e$ and $\nu_{\mu,\tau}/\bar{\nu}_{\mu,\tau}$. Therefore, we can obtain adiabatic/precession solutions using the same procedure listed in Sec. III B but with the replacements

$$|\nu_i\rangle \longrightarrow |\nu_i'\rangle \quad \text{and} \quad m_i^2 \longrightarrow m_i'^2. \quad (83)$$

Likewise, the conserved lepton numbers should be calculated in the $|\nu_i'\rangle$ basis instead of the $|\nu_i\rangle$ basis.

B. Effects of Virtual Charged Leptons

At very large matter density, virtual μ and τ states contribute to a higher order correction to neutrino refractive indices, and H^{matt} is found to be [4, 30, 31]

$$H^{\text{matt}} = \sqrt{2} G_F n_b \text{diag}(Y_e, 0, Y_\tau) \quad (84)$$

in the flavor basis, where $n_b Y_\tau$ gives the effective net τ lepton abundance. If the matter density is so large that

$$\sqrt{2} G_F n_b Y_\tau \gg |\kappa|, \quad (85)$$

we can again employ the corotating frame as in Eq. (77). Ignoring the rapidly-oscillating off-diagonal elements diagonalizes \tilde{H}_ω in the flavor basis in this corotating frame:

$$\tilde{H}_\omega^{\text{vac}} \simeq \frac{\omega}{\Delta m_{21}^2} \text{diag}(m_1''^2, m_2''^2, m_3''^2), \quad (86)$$

where

$$m_1''^2 \simeq c_{12}^2 m_1^2 + s_{12}^2 m_2^2, \quad (87a)$$

$$m_2''^2 \simeq c_{23}^2 (s_{12}^2 m_1^2 + c_{12}^2 m_2^2) + s_{23}^2 m_3^2, \quad (87b)$$

$$m_3''^2 \simeq s_{23}^2 (s_{12}^2 m_1^2 + c_{12}^2 m_2^2) + c_{23}^2 m_3^2 \quad (87c)$$

are the effective mass-squared value for the neutrino states

$$|\nu_1''\rangle \simeq |\nu_e\rangle, \quad (88a)$$

$$|\nu_2''\rangle \simeq |\nu_\mu\rangle, \quad (88b)$$

$$|\nu_3''\rangle \simeq |\nu_\tau\rangle. \quad (88c)$$

Therefore, the adiabatic/precession solution still obtains in the presence of both large electron and large effective tau abundances. In this case, however, the degeneracy among $\nu_e/\bar{\nu}_e$, $\nu_\mu/\bar{\nu}_\mu$ and $\nu_\tau/\bar{\nu}_\tau$ is completely broken. In this case, the adiabatic/precession solution is best obtained in the flavor basis. The conserved lepton numbers should also be calculated in the flavor basis.

Because the absolute neutrino masses are irrelevant for neutrino oscillations, in the inverted neutrino mass hierarchy case we can take $m_1 \simeq m_2^2 \simeq \Delta m_{\text{atm}}^2 > m_3^2 = 0$. When $n_b Y_\tau$ is large, from Eq. (87) it can be seen that the mass-squared eigenvalue for $|\nu_1''\rangle$ is always heavier than the mass-squared eigenvalues for $|\nu_2''\rangle$ and $|\nu_3''\rangle$, while the effective 23-mass-hierarchy, or the sign of

$$\Delta m_{32}''^2 \equiv m_3''^2 - m_2''^2, \quad (89)$$

depends on whether θ_{23} is larger or smaller than $\pi/4$. Similarly, for the normal neutrino mass hierarchy case, we can take $m_3^2 \simeq \Delta m_{\text{atm}}^2 > m_1^2 \simeq m_2^2 \simeq 0$, and again the effective 23-mass-hierarchy depends on whether θ_{23} is larger or smaller than $\pi/4$, although in a reversed fashion. According to the discussion in Sec. III C, the final energy spectra for $\nu_2''/\bar{\nu}_2''$ and $\nu_3''/\bar{\nu}_3''$ (and, therefore, the spectra for $\nu_\mu/\bar{\nu}_\mu$ and $\nu_\tau/\bar{\nu}_\tau$) interchange with each other when θ_{23} rotates from the first octant to the second octant. In other words, the final neutrino energy spectra can be sensitive to deviations from maximal 23-mixing. This can be illustrated using the toy model discussed in Ref. [29].

In this toy model the neutron star emits only ν_e and $\bar{\nu}_e$ with the same energy E_ν into a thick matter envelope where $n_b Y_\tau$ is large. In this model it is assumed also that $n_{\nu_e}/n_{\bar{\nu}_e} = 1 + \epsilon$ at the neutrino sphere with $\epsilon > 0$. If the neutrino gas follows the adiabatic/precession solution, then $P(\nu_e \rightarrow \nu_i'')$ and $P(\bar{\nu}_e \rightarrow \bar{\nu}_i'')$ must be either 0 or 1 except at swapping points (see Sec. III C). However, it is clear from the conservation of lepton numbers in the flavor basis that ν_e 's can not have been fully converted to other flavors. Because neutrino (instead of antineutrino) is the dominant species in the system, the spectral swaps occur in the neutrino sector. Therefore, $\bar{\nu}_e$'s are completely converted into antineutrinos of another flavor as $n_\nu^{\text{tot}} \rightarrow 0$. In this case, the precession ansatz in Eq. (43) is trivially satisfied as $n_\nu^{\text{tot}} \rightarrow 0$ in the corotating frame defined by

$$H_{\text{cor}} = H_{\omega_+}^{\text{vac}}, \quad (90)$$

where $H_{\omega_+}^{\text{vac}}$ is the vacuum term in the Hamiltonian for the neutrino mode with energy E_ν . In other words, both swapping points have collapsed into one which is located in the neutrino sector and at energy $E^s = E_\nu$. Following

the discussions in Sec. III C, we can use the conservation of lepton numbers in the flavor basis to find that the neutrino conversion probabilities are

$$P(\nu_e \rightarrow \nu_e) = \frac{\epsilon}{1 + \epsilon}, \quad (91a)$$

$$P(\nu_e \rightarrow \nu_\mu) = 0, \quad (91b)$$

$$P(\nu_e \rightarrow \nu_\tau) = \frac{1}{1 + \epsilon}, \quad (91c)$$

$$P(\bar{\nu}_e \rightarrow \bar{\nu}_e) = 0, \quad (91d)$$

$$P(\bar{\nu}_e \rightarrow \bar{\nu}_\mu) = 0, \quad (91e)$$

$$P(\bar{\nu}_e \rightarrow \bar{\nu}_\tau) = 1 \quad (91f)$$

for the inverted neutrino mass hierarchy and $\theta_{23} < \pi/4$. For the inverted neutrino mass hierarchy and $\theta_{23} > \pi/4$ we can obtain neutrino conversion probabilities which are similar to those in Eq. (91) but with $\nu_\mu \leftrightarrow \nu_\tau$ and $\bar{\nu}_\mu \leftrightarrow \bar{\nu}_\tau$. This is exactly what has been observed in the numerical calculations for the toy model at $r \simeq 400$ km (Fig. 2 in Ref. [29]).

V. CONCLUSIONS

We have developed a framework for studying collective three-flavor neutrino oscillations. Important techniques in studying collective two-flavor oscillations such as corotating frames can be applied readily to three-flavor scenarios in this framework. We have shown that the three-flavor adiabatic/precession solution obtains when both the precession ansatz and the adiabatic ansatz are satisfied. If the flavor evolution of a neutrino gas is described by the adiabatic/precession solution, the final neutrino energy spectra will exhibit the stepwise swapping phenomenon. We have shown that stepwise spectral swapping appears in a numerical example in which neutrinos are directly emitted from the neutrino sphere of a bare neutron star into vacuum. For this special example, because the neutrinos in μ and τ flavors are equally mixed and have identical energy spectra initially, the adiabatic/precession solutions for both the three-flavor and the two-flavor scenarios produce the same spectral swapping at the atmospheric neutrino mass-squared-difference scale. In more general cases, however, this may not be the case, and the full 3×3 mixing framework should be employed.

Strictly speaking, the adiabatic/precession solution obtains only when the CP -violating phase $\delta = 0$. This is

because, if $\delta \neq 0$, the unitary transformation matrix U connecting the flavor states and vacuum mass eigenstates is not real, and

$$U \rho_{\mathbf{p}}^* U^\dagger \neq (U \rho_{\mathbf{p}} U^\dagger)^* \text{ and } U \bar{\rho}_{\mathbf{p}}^* U^\dagger \neq (U \bar{\rho}_{\mathbf{p}} U^\dagger)^*. \quad (92)$$

As a result, Eqs. (4) and (7) become invalid in the vacuum mass basis, and all the following derivations are invalid. In practice, however, the adiabatic/precession solution may still be a good approximation even when δ is large. This is because $\theta_{13} \simeq 0$ and the transformation matrix U is almost real. In fact, numerical simulations in Ref. [28] show that, at least for the parameters employed in those simulations, varying the CP phase δ has little effect on the final neutrino energy spectra except for changing the relative mixing of μ and τ neutrino flavors. The possible effects of CP violation in stellar collapse have been discussed in a different context (see, e.g., Ref. [34]).

We also have demonstrated that the adiabatic/precession solution obtains even in the presence of a dominant matter background and a large mu-tau term. When the matter term is much larger than the vacuum mixing term, the presence of the ordinary matter only reshuffles the neutrino states in which the spectral swapping has the most dramatic manifestation. For the supernova environment, this means that the regime where collective neutrino oscillations occur is solely determined by the neutrino fluxes and does not depend sensitively on the matter density profile. This is in agreement with the previous analysis in two-flavor scenarios [16]. The supernova neutrino signals observed on earth will depend of course on the matter profile in the supernova. In part, this is because the MSW effect will modify the neutrino energy spectra subsequent to the collective oscillations discussed here. This dependence of neutrino signals on the matter profile can provide important information on the conditions deep in the supernova envelope [28, 35, 36].

Acknowledgments

This work was supported in part by DOE grants DE-FG02-00ER41132 at INT, DE-FG02-87ER40328 at UMN, NSF grant PHY-04-00359 at UCSD, and an IGPP/LANL mini-grant.

-
- [1] L. Wolfenstein, Phys. Rev. **D17**, 2369 (1978).
 - [2] L. Wolfenstein, Phys. Rev. **D20**, 2634 (1979).
 - [3] S. P. Mikheyev and A. Y. Smirnov, Yad. Fiz. **42**, 1441 (1985), [Sov. J. Nucl. Phys. **42**, 913 (1985)].
 - [4] G. M. Fuller, R. W. Mayle, J. R. Wilson, and D. N. Schramm, Astrophys. J. **322**, 795 (1987).

- [5] D. Nötzold and G. Raffelt, Nucl. Phys. **B307**, 924 (1988).
- [6] J. T. Pantaleone, Phys. Rev. **D46**, 510 (1992).
- [7] G. Sigl and G. Raffelt, Nucl. Phys. **B406**, 423 (1993).
- [8] G. M. Fuller, R. W. Mayle, B. S. Meyer, and J. R. Wilson, Astrophys. J. **389**, 517 (1992).
- [9] Y.-Z. Qian, G. M. Fuller, G. J. Mathews, R. W. Mayle,

- J. R. Wilson, and S. E. Woosley, Phys. Rev. Lett. **71**, 1965 (1993).
- [10] S. Samuel, Phys. Rev. **D48**, 1462 (1993).
- [11] V. A. Kostelecky and S. Samuel, Phys. Rev. **D52**, 621 (1995), hep-ph/9506262.
- [12] S. Pastor, G. G. Raffelt, and D. V. Semikoz, Phys. Rev. **D65**, 053011 (2002), hep-ph/0109035.
- [13] S. Pastor and G. Raffelt, Phys. Rev. Lett. **89**, 191101 (2002), astro-ph/0207281.
- [14] A. B. Balantekin and H. Yüksel, New J. Phys. **7**, 51 (2005), astro-ph/0411159.
- [15] G. M. Fuller and Y.-Z. Qian, Phys. Rev. **D73**, 023004 (2006), astro-ph/0505240.
- [16] H. Duan, G. M. Fuller, and Y.-Z. Qian, Phys. Rev. **D74**, 123004 (2006), astro-ph/0511275.
- [17] H. Duan, G. M. Fuller, J. Carlson, and Y.-Z. Qian, Phys. Rev. **D74**, 105014 (2006), astro-ph/0606616.
- [18] H. Duan, G. M. Fuller, J. Carlson, and Y.-Z. Qian, Phys. Rev. Lett. **97**, 241101 (2006), astro-ph/0608050.
- [19] S. Hannestad, G. G. Raffelt, G. Sigl, and Y. Y. Y. Wong, Phys. Rev. **D74**, 105010 (2006), astro-ph/0608695.
- [20] G. G. Raffelt and G. G. R. Sigl, Phys. Rev. **D75**, 083002 (2007), hep-ph/0701182.
- [21] H. Duan, G. M. Fuller, J. Carlson, and Y.-Z. Qian, Phys. Rev. **D75**, 125005 (2007), astro-ph/0703776.
- [22] H. Duan, G. M. Fuller, J. Carlson, and Y.-Z. Qian, Phys. Rev. Lett. **99**, 241802 (2007), arXiv:0707.0290 [astro-ph].
- [23] G. L. Fogli, E. Lisi, A. Marrone, and A. Mirizzi, JCAP **0712**, 010 (2007), arXiv:0707.1998 [hep-ph].
- [24] A. Esteban-Pretel, S. Pastor, R. Tomas, G. G. Raffelt, and G. Sigl, Phys. Rev. **D76**, 125018 (2007), arXiv:0706.2498 [astro-ph].
- [25] G. G. Raffelt and A. Y. Smirnov, Phys. Rev. **D76**, 081301(R) (2007), arXiv:0705.1830 [hep-ph].
- [26] G. G. Raffelt and A. Y. Smirnov, Phys. Rev. **D76**, 125008 (2007), arXiv:0709.4641 [hep-ph].
- [27] H. Duan, G. M. Fuller, and Y.-Z. Qian, Phys. Rev. **D76**, 085013 (2007), arXiv:0706.4293 [astro-ph].
- [28] H. Duan, G. M. Fuller, J. Carlson, and Y.-Z. Qian, Phys. Rev. Lett. **100**, 021101 (2008), arXiv:0710.1271 [astro-ph].
- [29] A. Esteban-Pretel, S. Pastor, R. Tomas, G. G. Raffelt, and G. Sigl (2007), arXiv:0712.1137 [astro-ph].
- [30] F. J. Botella, C. S. Lim, and W. J. Marciano, Phys. Rev. **D35**, 896 (1987).
- [31] E. Roulet, Phys. Lett. **B356**, 264 (1995), hep-ph/9506221.
- [32] B. Dasgupta and A. Dighe (2007), arXiv:0712.3798 [hep-ph].
- [33] W.-M. Yao et al., J. Phys. **G33**, 1 (2006).
- [34] A. B. Balantekin, J. Gava, and C. Volpe (2007), arXiv:0710.3112 [astro-ph].
- [35] R. C. Schirato and G. M. Fuller (2002), astro-ph/0205390.
- [36] C. Lunardini, B. Mueller, and H. T. Janka (2007), arXiv:0712.3000 [astro-ph].